Cyclic loading of helical pile as anchor for floating windturbines : centrifuge tests

Luc Thorel, Ismat El Haffar, Semaan Maatouk, José Antonio Schiavon, Cristina Tsuha

CYCLIC LOADING OF HELICAL PILE AS ANCHOR FOR FLOATING WINDTURBINES: CENTRIFUGE TESTS

Luc THOREL, Univ. Gustave Eiffel, GERS-GMG, F-44344 Bouguenais-Nantes, France, +33240845808, luc.thorel@univ-eiffel.fr
Ismat EL HAFFAR, Fugro GeoConsulting, Bruxelles, Belgique, i.elhaffar@fugro.com.
Semaan MAATOUK, Univ. Gustave Eiffel, GERS-GMG, France, semaan.matouk@univ-eiffel.fr
Jose Antonio SCHIAVON, Instituto Tecnológico de Aeronáutica, Sao Jose, Brasil, schiavon@ita.br
Cristina TSUHA, Univ Sao Paulo, Sao Carlos, Brasil, chctsuha@sc.usp.br

ABSTRACT

Helical piles are currently used in several countries for onshore applications. In the perspective of the development of floating wind turbines, helical pile should be used as an anchoring system. The understanding of the behavior of this anchoring system is investigated under cyclic loading. Installation phase in a saturated sand, monotonic tension and cyclic behavior are analyzed, based on small scale (1/10) centrifuge models. After a presentation of the experimental device, some parameters are investigated, such as the installation torque for two rotation rates and the displacements under cyclic loading.

Keywords: helical pile, mono-helix, tension loading, cyclic loading

NOTATIONS

d	shaft diameter
D	Helix diameter
Q_c	Axial cyclic load amplitude
Q_m	Mean axial cyclic loading
Q_T	Ultimate tension capacity of the pile
δ	Vertical displacement

INTRODUCTION

Offshore Wind Turbines (OWT) follow an exponential development since 1991 (Orsted 2017) as a new source of “green and blue” energy. If today the market is devoted to OWTs fixed on the underwater ground, the trends of the future concern deeper water and floating solutions (Butterfield et al. 2005), such as the prototypes recently developed in Europe (e.g. Floatgen, Hywind/Equinor, Windfloat/EDP, Eolink), North America (e.g. Aqua ventus) or Japan (e.g. Hibiki, NEDO Channel 2019).

Catenary mooring lines are used for the existing Floating Wind Turbines (FWT). This system is based on the use of free hanging lines fixed at the seabed with the use of drag anchors or suction anchors. The mass of the catenary line is the key aspect to the stability of this system. Some studies have treated the development and optimization of the use of such type of mooring system (Goldschmidt and Muskulus 2015, Brommundt et al. 2012). As an alternative of the use of the catenary lines, Tension Leg Platform (TLP) system has been proposed for deeper water. This system is based on the use of tension steel leg fixed by piles or anchors at the seabed. A perspective use of helical pile for the fixation of these types of structures presents many advantages in comparison with the conventional driven piles: (1) Reduced noise pollution in comparison with pile-driving method, (2) Easy unscrewing which will aid the decommissioning of the structure at the end of its service (Byrne and Houlsby 2015). A major practical advantage also of the use of helical pile is that the capacity of these piles can be predicted from the torque measurement during installation (Tsuha and Aoki 2010).

The tension and compression static behavior of helical piles has been well treated in the literature (Ghaly et al. 1991, Gavin et al. 2014, Merifield 2011, Elsherbiny and El Naggar 2013, Ghaly and Clemence 1998, George et al. 2019, Hao et al. 2018). On the other hand, fewer studies exist on the cyclic behavior of helical piles (Schiavon 2016, Schiavon et al. 2017, El Sharnouby and El Naggar 2012, Wada et al. 2017, Newgard et al. 2015). The focus of previous research on helical pile was

oriented to onshore application and the saturation of the soil was not a priority. Here, centrifuge tests in saturated Hostun HN38 sand, have been performed on single-helix helical model pile in order to study the cyclic behavior.

METHODOLOGY

Centrifuge modeling

Centrifuge modeling is used here on small scale models installed in a macro gravity field allowing for the replication of stress state occurring within prototype soil. The Ifsttar's geotechnical centrifuge (Fig.1) is a 200×g.ton machine with a radius of 5.5 m that allows to carry 2000 kg at a g-level of 100.

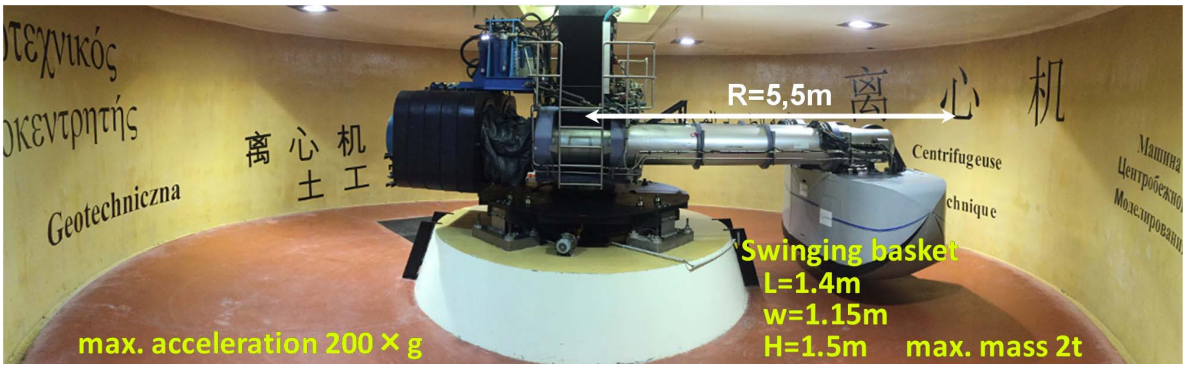

Fig.1 University Gustave Eiffel**'s geotechnical centrifuge**

The tests presented are carried out on 1/10 scale piles scaled at 10 times the Earth's gravity (10×g). In this case, the main scaling laws (Garnier et al. 2007) used to link the prototype (full scale) to the (small-scale) centrifuge model are listed in Table 1: for instance $x^* = x^{model}/x^{prototype}$.

Table 1. Scaling law for different parameters (with *N* = 10)

Parameter	Notation	Unit	Scaling factor
Distance	x^*	L	1/N
Stress	σ^*	M/LT^2	1
Density	ρ^*	M/L^3	1
Gravity	g^*	L/T^2	N
Displacement	u^*	L	1/N
Strain	ε^*	-	1
Velocity	v^*	L/T	1
Acceleration	a^*	L/T^2	N
Frequency	f^*	1/T	N
Force	F^*	ML/T^2	$1/N^2$
Unit weight	γ^*	M/L^2T^2	1
Mass	m^*	M	$1/N^3$
Torque	T^*	ML^2/T^2	$1/N^3$

Model soil

The model soil consists of Hostun HN38 sand (Table 2) with a relative density of 89% obtained by air pluviation into a rectangular strongbox of internal dimensions 1200 mm × 800 mm × 360 mm (length × width × depth).

Table 2: Characteristics of Hostun sand HN38 (Schiavon et al. 2017)

Sand	d_{60}/d_{10}	d_{50} (µm)	$\rho_{d\,min}$ (kg/m^3)	$\rho_{d\,max}$ (kg/m^3)
Hostun HN38	1.97	120	1223	1565

Once the pluviation finished, the strongbox is connected to a water tank by the underside to progressively saturate the sand mass. The final water table elevation is 4 cm above the level of the sand surface.

Model pile and experimental campaign

The model pile is a single helix rigid steel pile with a shaft diameter of d = 10 mm, helical plate diameter of D = 33 mm, a helix pitch of 9.7 mm and helix thickness of 1.5 mm. The corresponding prototype pile is then 100 mm in shaft diameter, 330 mm of helix diameter, 97 mm of helix pitch and helix thickness of 15 mm. The experimental set-up presented in Fig. 2 permits in-flight installation and loading of the pile. The pile is installed with a controlled rotation rate up to a helix embedment of 7.4D. The vertical jacking rate is also controlled in order to ensure a penetration of one pitch per revolution of the pile. A load-torque sensor is placed at the head of the pile and permits the measurement of the force and the torque applied at the pile during the installation and the following loading tests.

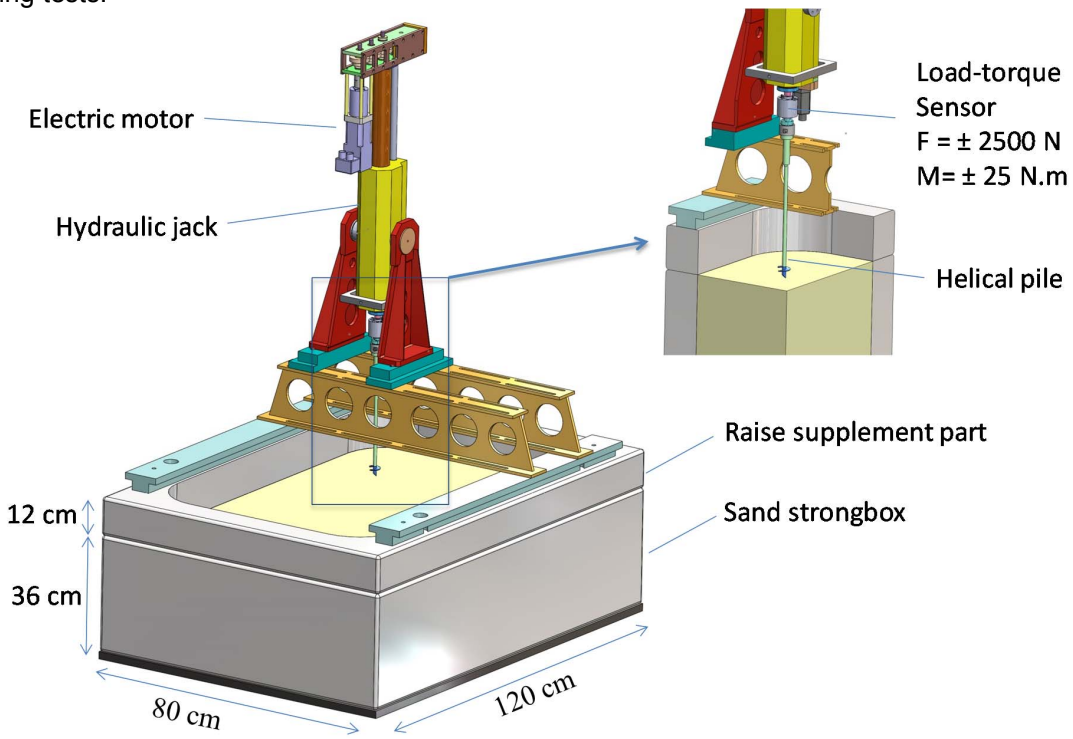

Fig. 2: Experimental set-up (inner dimensions)

The cyclic testing from installation, loading, and pull-out followed the typical procedure outlined in Schiavon et al. (2018). Each cyclic loading was conducted up to a vertical accumulated displacement of 10%D, or at least for a minimum number of cycles N = 1000. The cyclic loading was controlled in force performing a constant-amplitude sine function. The characterizing parameters of cyclic loading Q_m (mean axial cyclic load) and Q_c (axial cyclic load amplitude) are defined by:

$$Q_m = (Q_{max} + Q_{min})/2 \quad [1]$$

$$Q_c = (Q_{max} - Q_{min})/2 \quad [2]$$

in which, Q_{max} and Q_{min} are the maximum and minimum axial load values applied to the model pile head during cycling (Fig.3).

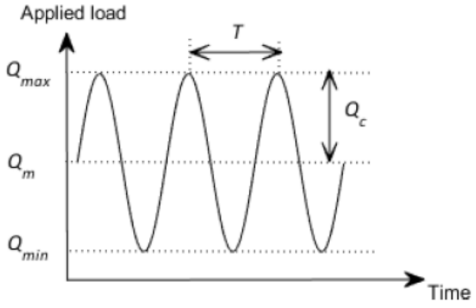

Fig. 3: Load controlled cyclic loading

A set of 18 cyclic tests with variable amplitudes has been performed in this study (Maatouk, 2019), using a frequency of 0.3 or 0.4 Hz. The initial Q_m is reached under a displacement-controlled movement of the helical pile, and then the cyclic loading is force-controlled.

RESULTS

Effect of installation rotation speed in saturated sand

In the field (at full scale), classical rotation rate during helical pile installation is generally lower than 20 rpm. Here the question of quasi-static or dynamic loading, locally on the helix, is raised as the scaling laws (e.g. Garnier et al. 2007) suggest that in case of non-quasi-static loading, the viscosity on the pore fluid should be increased by a factor 10. Another point is about the pore pressure dissipation: is the behavior of the soil in the vicinity of the helix under drained or undrained conditions? In order to estimate the potential effect of the rotation rate of the helical pile during the installation, two rotation rates of installation have been tested: 1 and 13 rpm. Taking into account the geometry of the pile (d = 10 mm and D = 33 mm) and the rotation rates, the relative helix/sand grain local shear velocity varies from the range 0.52-1.7 mm/s to the range 6.8-22 mm/s.The installation phase shows for the torque calculated over the deepest 3D (T_{3D}) a variation of 15% between the 2 tests (Fig.4), while the difference between the maximum tensile loads is less than 4% (Fig.5). Regarding the dimensionless torque factor ($Q_T.D/T_{3D}$) suggested by Byrne and Houlsby (2015), it increases from 4.80 to 5.45 (13% of variation) when increasing the rotation rate by 13.

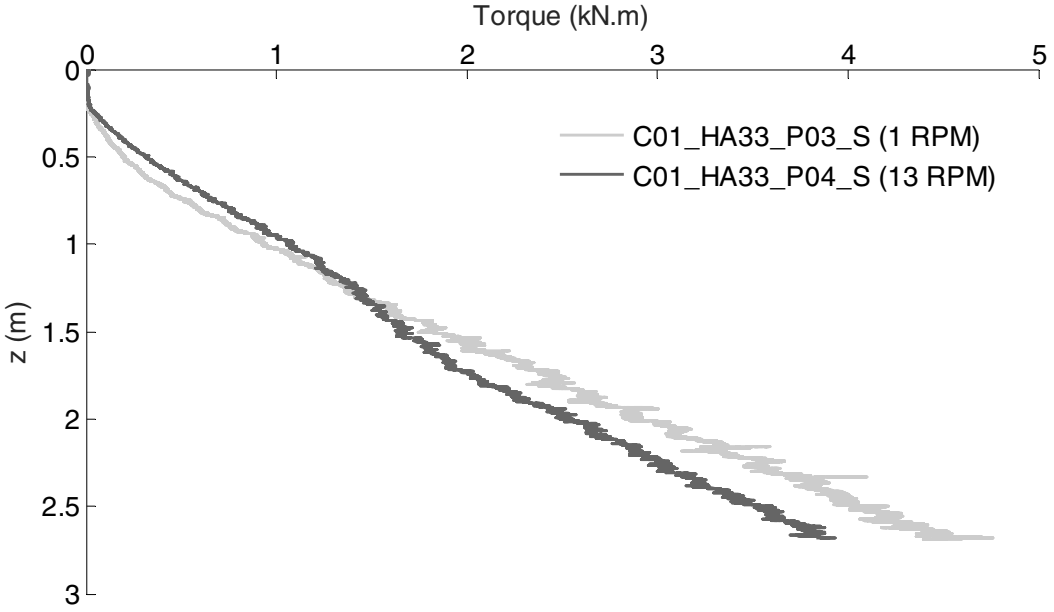

Fig. 4: Installation torque against depth for rotation rate of 1 and 13 rpm.

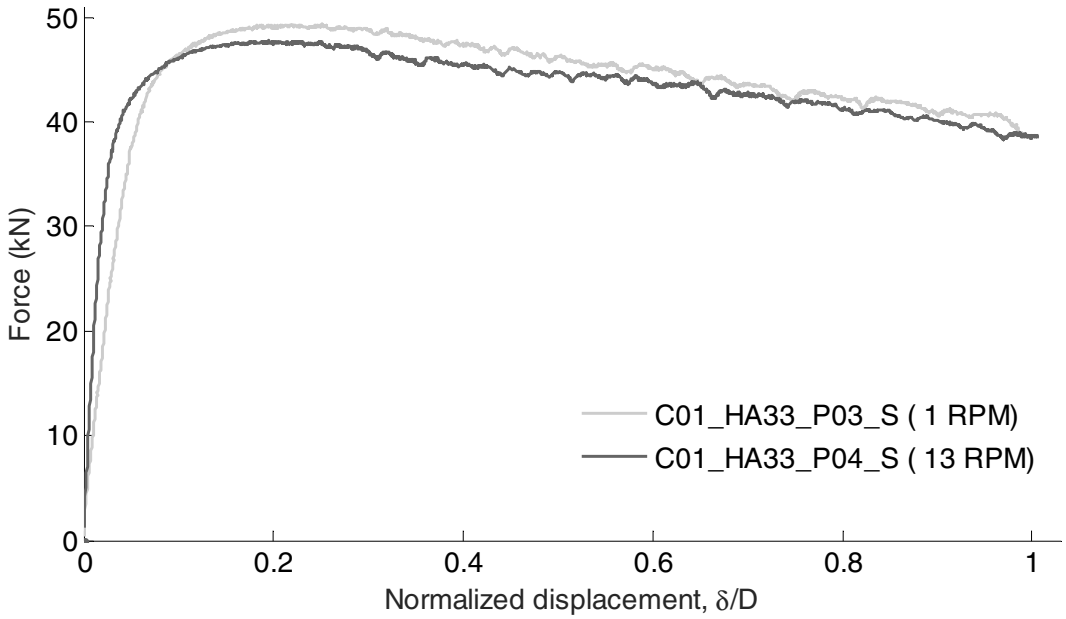

Fig. 5: Tension test for rotation rate of 1 and 13 rpm.

It can be concluded that, even if a difference is observed on the torque profiles, the whole behavior in tension is not affected so much. Of course, additional tests with different rotation rates should be useful for a better understanding of the phenomena, including pore pressure measurements.

Stability diagram

The study of foundation systems subjected to cyclic loads must include not only its capacity but also its displacements over time. Poulos (1988) proposed a stability diagram to evaluate the response of regular piles under cyclic loading: the axes are Qc/Q_T versus Qm/Q_T, where Q_T is the monotonic ultimate resistance in tension (Fig.5). Tsuha et al. (2012) recommend a definition of the stability zones according to the displacement rate. They are classified into three zones: stable, unstable and metastable.

- A Stable (S) zone, where axial displacements stabilize or accumulate very slowly for a considerable number of cycles greater than 1000.
- An Unstable (U) zone, where displacements accumulate rapidly until reaching the failure for a small number of cycles less than 100.
- An intermediate Meta-Stable (M) zone, where displacements accumulate at moderate rates until reaching the failure between 100 and 1000 cycles.

In this cyclic diagram (Fig.6), the theoretically allowable loading is inside the hatched triangle below the diagonal corresponding to the safety factor equal to 1. All the performed tests are in the one-way tensile cyclic loading zone. Based on the anchor head displacement, there are ten cyclic tests where the displacement of the anchor head accumulates slowly and does not reach the displacement limit of 10% of the helix diameter (33 mm in prototype scale) during the 1000 cycles and can be classified as stable (S). Three cyclic tests are classified as Unstable (U) in which the displacement increases rapidly reaching a limiting value of 10%*D* during the first 100 cycles, and five cyclic tests are classified as Meta-Stable (M) in which the anchor head reaches a displacement of 10%*D* between the 100 and 1000 cycles.

The stable, Meta-Stable and Unstable zones cannot be precisely delimited due to the low number of tests performed but a safety factor of 1.6 can be defined during the design of the studied pile (d = 100 mm and D = 330 mm in prototype scale) to insure a stable response of the pile. Additional tests are necessary to more accurately investigate the boundaries between the 3 zones.

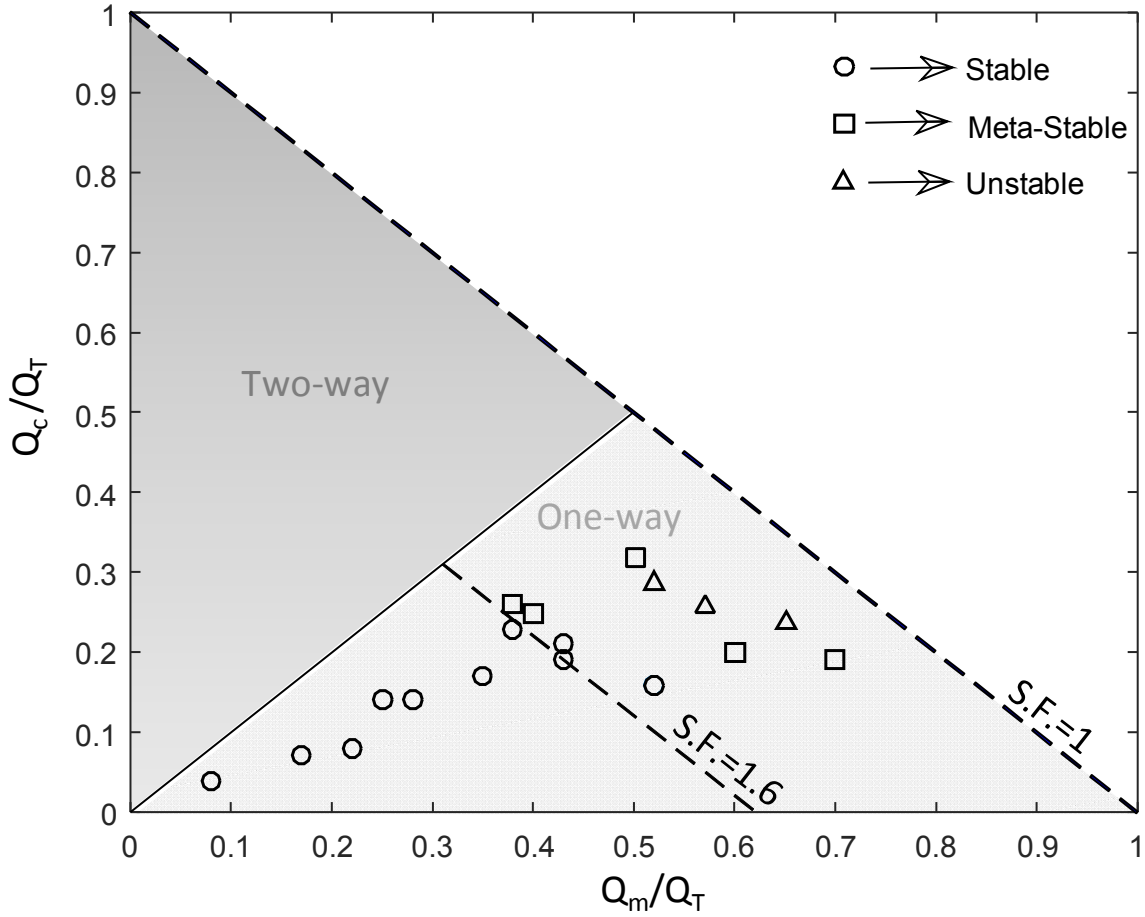

Fig. 6: Cyclic interaction diagram.

CONCLUSIONS

Centrifuge tests on 1/10 scale models of single-helix anchor have been performed, including in-flight installation phase and tension loading. If the installation torque appears 15% smaller for rotation rate 13 times higher the ultimate monotonic resistance is only 4% smaller, which is in the range of classical natural variability, showing almost no effect of the installation rotation rate on the tension resistance. A set of 18 cyclic tests has permitted to identify the limits between the stable, metastable and unstable zones in the stability diagram, suggesting a possible safety factor of 1.6.

ACKNOWLEDGEMENTS

The authors wish to thank WEAMEC (Projects REDENV-EOL and JE-CORECT), the Region Pays de Loire, Nantes Metropoles and CARENE for their financial support to the project grants, within the context of which this study has been conducted. Special thanks to the Univ. Gustave Eiffel Centrifuge team for its technical support and assistance during the centrifuge experimental campaign.

REFERENCES

Aqua Ventus. 2019. Offshore Wind Advanced Technology. Demonstration Projects. https://www.energy.gov/eere/wind/offshore-wind-advanced-technology-demonstration-projects. Accessed 19-7-7.

Brommundt, M., Krause, L., Merz, K., and Muskulus, M. 2012. Mooring system optimization for floating wind turbines using frequency domain analysis. Energy Procedia 24: 289-296.

Butterfield, S., Musial, W., Jonkman, J., and Sclavounos, P. 2005. Engineering Challenges for Floating Offshore Wind Turbines. Proceedings, Copenhagen Wind Conference, Copenhagen, October 26-28, pp. 1-10.

Byrne, B.W. and Houlsby, G.T. 2015. Helical piles: an innovative foundation design option for offshore wind turbines. Phil. Trans. R. Soc. A 373: 20140081.

EDP. 2019. Windfloat – Innovation at EDP. Website. https://www.edp.com/en/windfloat. Accessed 19-7-7.

El Sharnouby, M.M. and El Naggar, M.H. 2012. Field investigation of axial monotonic and cyclic performances of reinforced helical pulldown micropiles. Canadian Geotechnical Journal, 49(5) 560-573.

Elsherbiny, Z.H., and El Naggar, M.H. 2013. Axial compressive capacity of helical piles from field tests and numerical study. Canadian Geotechnical Journal, 50(12) 1191-1203.

Eolink. 2019. Cost effective floating wind parks. Website. http://eolink.fr/en/. Accessed 19-7-7.

Equinor. 2019. How Hywind works. Website. https://www.equinor.com/en/what-we-do/hywind-where-the-wind-takes-us/hywind-up-close-and-personal.html. Accessed 19-7-7.

Floatgen. 2019. Project Floatgen. Website. https://floatgen.eu/fr. Accessed 19-7-7.

Garnier J., Gaudin C., Springman S.M., Culligan P.J., Goodings D., Konig D., Kutter B., Phillips R., Randolph M.F., and Thorel L. 2007. Catalogue of scaling laws and similitude questions in geotechnical centrifuge modelling. Int. J. Physical Modelling in Geotechnics, 7(3), pp. 1-24.

Gavin, K., Doherty, P., and Tolooiyan, A. 2014. Field investigation of the axial resistance of helical piles in dense sand. Canadian Geotechnical Journal, 51(11), pp. 1343-1354.

George, B.E., Banerjee, S., and Gandhi, S.R. 2019. Helical Piles Installed in Cohesionless Soil by Displacement Method. International Journal Geomechanics. 19(7), pp. 04019074.

Ghaly, A. and Clemence, S.P. 1998. Pullout performance of inclined helical screw anchors in sand. Journal of Geotechnical and Geoenvironmental Engineering, 124(7), pp. 617- 627.

Ghaly, A., Hanna, A., and Hanna, M. 1991. Installation torque of screw anchors in dry sand. Soils Foundations, 31(2), pp. 77-92.

Goldschmidt, M. and Muskulus, M. 2015. Coupled mooring systems for floating wind farms. Energy Procedia, 80, pp. 255-262.

Hao, D., Wang, D., O'Loughlin, C.D., and Gaudin, C. 2018. Tensile Monotonic capacity of helical anchors in sand: interaction between helices. Canadian Geotechnical Journal, 56(10), pp. 1534-1543.

Maatouk, S. 2019. Behavior of helical piles used as a floating wind turbine anchor: physical modelling in a centrifuge. Master thesis "Geomechanics, Civil Engineering and Risks". University Grenoble Alpes, 99 p.

Merifield, R.S. 2011. Ultimate Uplift Capacity of Multiplate Helical Type Anchors in Clay. Journal of Geotechnical and Geoenvironmental Engineering, 137(7), pp. 704-716.

NEDO Channel. 2019. The Birth of Hibiki, The Next-Generation Floating Offshore Wind Turbine System. Video. https://www.youtube.com/watch?v=D_JMikMXnUg. Accessed 19-7-7.

Newgard, J.T., Schneider, J.A., and Thompson D.J. 2015. Cyclic response of shallow helical anchors in a medium dense sand. Proceedings of the Third Frontiers in Offshore Geotechnics, Oslo, June 10-12, V. Meyer, Editor, Taylor & Francis Group, pp. 913-918.

Orsted. 2017. The world's first offshore wind farm is retiring. Website. https://orsted.com/en/Media/Newsroom/News/2017/03/The-worlds-first-offshore-wind-farm-is-retiring. Accessed 19-7-7.

Poulos, H.G. 1988. Cyclic stability diagram for axially loaded piles. ASCE J. Geotechnical Engineering Division, 114(8), pp. 877-895.

Schiavon, J.A. 2016. Behaviour of helical anchors subjected to cyclic loadings. PhD thesis. University of São Paulo and LUNAM University, 300 p.

Schiavon, J.A., Tsuha, C.H.C., and Thorel, L. 2017. Cyclic and post-cyclic monotonic response of a single-helix anchor in sand. Géotechnique Letters, 7(1), pp. 11-17.

Schiavon, J.A., Tsuha, C.H.C., Neel, A., and Thorel, L. 2018. Centrifuge modelling of a helical anchor under different cyclic loading conditions in sand. International Journal of Physical Modelling in Geotechnics 2019 19(2), pp. 72-88.

Tsuha, CHC and Aoki, N. 2010. Relation between installation torque and uplift capacity of deep helical piles in sand. Canadian Geotechnical Journal, 47(6), pp. 635-647.

Tsuha, C.H.C., Foray, P.Y., Jardine, R.J., Yang, Z.X., Silva, M., and Rimoy, S. 2012. Behaviour of displacement piles in sand under cyclic axial loading. Soils and Foundations, 52(3), pp. 393-410.

Wada, M., Tokimatsu, K. Maruyam, S., and Sawaishi, M. 2017. Effects of cyclic vertical loading on bearing and pullout capacities of piles with continuous helix wing. Soils and Foundations, 57(1), pp. 141-153.